Brain heparanase expression is up-regulated during postnatal development and hypoxia-induced neovascularization in adult rats.

Fabrice P Navarro, Raafat P Fares, Pascal E Sanchez, Jérémie Nadam, Béatrice Georges, Colette Moulin, Anne Morales, Jean-Marc Pequignot, Laurent Bezin

Brain heparanase expression is upregulated during postnatal development and hypoxia-induced neovascularization in adult rats

Fabrice P. Navarro,[1,2,3] Raafat P. Fares, [1,2,3,†] Pascal E. Sanchez, [1,2,3,†] Jérémie Nadam, [1,2,3] Béatrice Georges, [1,2,3] Colette Moulin, [1,2,3] Anne Morales, [1,2,3] Jean-Marc Pequignot, [1,2,3] and Laurent Bezin [1,2,3,*]

[1] Université de Lyon, Lyon, F-69003, France; Université Claude Bernard Lyon 1, Villeurbanne, F-69622, France; Centre National de la Recherche Scientifique UMR 5123, laboratory of Integrative Cellular and Molecular Physiology, Villeurbanne, F-69622, France.

[2] Institut Fédératif de Recherche 41, Villeurbanne, F-69622, France.

[3] CTRS-IDÉE, Hospices Civils de Lyon, Lyon, F-69003, France.

[†] These authors contributed equally to the work and are listed in alphabetical order.

*Corresponding author : **Laurent Bezin**

e-mail: laurent.bezin@univ-lyon1.fr

Phone : +33 472 445 841 *Fax* : +33 472 431 172

Abstract

Heparanase is an endo-β-D-glucuronidase which specifically cleaves extracellular and cell surface heparan sulphates (HS) at intrachain sites. Its enzymatic activity is strongly implicated in cell dissemination associated with tumor metastasis and inflammation. Indeed, heparanase gene is expressed in various tumors and its over-expression is correlated with increased tumor vascularity and metastatic potential of tumor cells. However, heparanase expression in non-invasive and non-immune tissue, including brain, has received less attention. Using RT-qPCR, western blot and histological analysis, we demonstrate in the adult rat that heparanase transcript is differentially expressed according to brain area, and that heparanase protein is mainly detected in neurons. Furthermore, we provide evidence that heparanase transcript and protein reach their greatest levels at early postnatal stages, in particular within the neocortex characterized by intensive structural plasticity. Using the *in vitro* model of PC12-induced neuronal differentiation, we suggest that developmental regulation of heparanase may coincide with axonal and dendritic pathfinding. At adulthood, we demonstrate that the increased heparanase transcript level correlates in the hippocampus with enhanced angiogenesis following repeated hypoxia exposures. Taken together, our results emphasize the potential importance of heparanase in brain homeostasis, both during development and adaptative responses to severe environmental challenges.

Keywords: angiogenesis; environmental enrichment; hippocampus; neocortex; neuronal differentiation; VEGF.

Running title: Neuronal expression of heparanase

Introduction

Heparan sulfate (HS) chains present on HS proteoglycans (HSPGs) are abundantly found in the extracellular matrix (ECM) of the brain (Lander 1993, Margolis & Margolis 1993). Due to their binding capacities (Deepa *et al.* 2004, Lortat-Jacob *et al.* 2002, Rapraeger 1995, Taipale & Keski-Oja 1997), HS chains sequester numerous bioactive molecules, such as growth factors (Esko & Selleck 2002, Gallagher 2001, Lindahl *et al.* 1998, Lyon & Gallagher 1998, Taipale & Keski-Oja 1997, Turnbull *et al.* 2001). Heparanase is a mammalian endo-β-D-glucuronidase involved in degrading HS chains (Marchetti & Nicolson 2001, Okada *et al.* 2002, Pikas *et al.* 1998, Thunberg *et al.* 1982), and can thus liberate and increase the availability of growth factors (Ishai-Michaeli *et al.* 1990, Parish 2006) known to play important roles in brain plasticity.

Heparanase gene sequence has been determined in various mammalian species, including human (Hulett *et al.* 1999, Kussie *et al.* 1999, Toyoshima & Nakajima 1999, Vlodavsky *et al.* 1999), rat (Hulett et al. 1999) and mouse (Miao *et al.* 2002). Heparanase (EC:3.2.1-) is synthesized and secreted as a latent 65 kDa precursor and, as such, is retained at pericellular sites by binding to cell surface HS components (Gingis-Velitski *et al.* 2004, Goldshmidt *et al.* 2001). The full-length 65 kDa heparanase pro-enzyme undergoes proteolytic processing yielding an active heterodimer enzyme composed of 50 and 8 kDa polypeptides (Fairbanks *et al.* 1999, Levy-Adam *et al.* 2003, McKenzie *et al.* 2003, Nardella *et al.* 2004).

In brain tissue, heparanase expression has mainly been studied in the context of tumor progression, and was attributed to invasive cells (Hulett et al. 1999, Marchetti *et al.* 2000, Nakajima *et al.* 1988, Parish *et al.* 1987, Parish *et al.* 2001, Vlodavsky et al. 1999). Recently, heparanase transcript has been shown to be constitutively expressed in the brain of hypoxia-tolerant blind mole rat (Nasser *et al.* 2005), in neurons and white matter glia of rat spinal cord (Zhang *et al.* 2006), and in cultured astrocytes (Marchetti et al. 2000). Because (i) degradation of HS chains by heparanase appears to affect the integrity and functional state of tissues (Nasser et al. 2005), (ii) HSPGs play a critical role in developmental processes (Perrimon & Bernfield 2000), and (iii) transcripts of enzymes that catalyze polymerization of HS chains are up-regulated during postnatal development (Inatani & Yamaguchi 2003), we hypothesized that brain expression of heparanase is profoundly altered throughout lifespan.

Furthermore, we explored whether brain expression of heparanase could be upregulated in adult rats under physiological situations associated with structural remodeling, such as hypoxia acclimatization (Miyamoto *et al.* 2005, Patt *et al.* 1997) and enriched housing (Nithianantharajah & Hannan 2006, Stranahan *et al.* 2006, van Praag *et al.* 2000). In these different physiological conditions, we thus analysed for the first time heparanase gene expression in distinct brain areas at both transcript level (using RT- quantitative PCR) and protein level (using histological and immunoblotting approaches).

Materials and methods

Design of animal studies

Animals. All animal procedures were in compliance with the guidelines of the European Union (directive 86/609), taken in the French law (decree 87/848) regulating animal experimentation. All efforts were made to minimize animal suffering and to reduce the number of animals used. Sprague-Dawley male rats (Harlan, France) were used throughout the experiments. They were housed in approved facilities, at 21 ± 1°C under diurnal lighting conditions (lights on from 06:00 to 18:00). Rats used during the first 3 weeks (w) of life arrived at 1 day old with foster dams. Rats used at 3 and 12 month (mo) old arrived at the animal facility 3 weeks before the experiments started. Pups were maintained in groups of 10 with their foster dam until postnatal day (d) 21. Older rats (3 mo and 12 mo) were maintained in groups of 5 in plastic cages. All rats (foster dams and adult rats) had free access to food and water.

Experiment 1: Determination of basal expression of heparanase in different brain structures. Transcript levels of heparanase were determined in the hippocampus, the neocortex, the olfactory bulb, the dorsal part of thalamus and the hypothalamus of rats sacrificed at 3 mo (n=5). Localization of heparanase protein was performed on paraformaldehyde-fixed tissue in rats (n=5) of the same age.

Experiment 2: Determination of heparanase expression throughout postnatal development and ageing. Analysis of heparanase gene expression was performed in rats sacrificed at 2 d (n=8), 5 d (n=6), 1 w (n=8), 2 w (n=5), 3 w (n=5), 3 mo (n=5) and 12 mo (n=5). Transcript levels of heparanase

were determined in the hippocampus, the neocortex, and the olfactory bulb at all ages mentioned. Western blot analysis of immunoreactive heparanase was performed in the neocortex of the rats sacrificed at 2 d, 2 w, 3 mo and 12 mo. Localization of heparanase protein was performed on paraformaldehyde-fixed tissue in rats sacrificed at 5 d (n=5), 3 mo (n=5) and 12 mo (n=5).

Experiment 3: Effect of hypoxia preconditioning on heparanase mRNA expression. Hypoxia preconditioning consisted in 1 (H1) or 3 (H3) hypoxic exposures in 3 month-old rats. Hypoxia was realized by introducing rats within a chamber (Biospherix), the oxygen (O_2) proportion of which decreased progressively from 21% to 8% in one hour. Each hypoxia exposure was maintained at 8% O_2 during 6 hours. O_2 proportion was automatically regulated by the Pro-Ox system (Biospherix). In the H3 protocol, the 3 hypoxia exposures were carried out 4 days apart to facilitate the animal recovery. Transcript levels of heparanase were determined in the hippocampus of rats sacrificed immediately after the last hypoxic exposure, and then 1, 2 and 8 days later (Controls, n=4; H1 and H3, n=4 in each group at each time post-hypoxia considered). The surface area occupied by brain capillaries was measured in the hippocampus of rats sacrificed 3 days after the last hypoxic exposure (Controls, H1, and H3; n=3 in each group), by use of immunohistological detection on paraformaldehyde-fixed tissue of CD34, a vascular endothelial marker (Vaquero *et al.* 2000, Young *et al.* 1995).

Experiment 4: Effect of enriched housing on heparanase mRNA expression. Enriched environment "EE" consisted in housing 12 rats in a plexiglass box (80 cm x 80 cm x 40 cm) with plastic tubes, tunnels, ladders, 3 running wheels and toys that were rearranged 3 times a week during cage cleaning to encourage exploratory behavior and provide ongoing novelty to their environment. Standard environment "SE" consisted of housing 6 rats in polycarbonate boxes (40 cm x 20 cm x 18 cm). Transcript levels of heparanase were determined in the hippocampus of rats (n=18), housed for 7 weeks [from weaning (21 days) to day 70], either in EE (n=9) or in SE (n=9). The effect of EE on hippocampal plasticity was verified by measuring neurogenesis at day 70, in rats housed in EE (n=3) or SE (n=3). Therefore, 60 day-old rats received 5 consecutive injections of 5'-bromo-deoxyuridine (BrdU; Sigma B5002), at 17:00 the first day, and at 12:00 and 17:00 the two following days. Rats were transcardially perfused 10 days after the first BrdU injection with 4% paraformaldehyde solution

for counting of BrdU-incorporating cells within the dentate gyrus of the hippocampal formation, an active neurogenic zone in adults (Stranahan et al. 2006, van Praag et al. 2000).

In vitro experimental design

Cell culture. Rat PC12 cells were maintained in tissue culture flasks (175 cm²) in a humidified (90%) atmosphere of 95% air/ 5% CO_2 at 37°C. The medium ("PC12 complete medium", PC12CM) consisted of Dulbecco's modified Eagle's medium (DMEM, Eurobio # CM1DME60K), supplemented with 7% heat-inactivated horse serum, 7 % newborn bovine serum and antibiotics (80 units/mL penicillin and 80 mg/mL streptomycin). Culture medium was changed every other day.

Experiment 5: Correlation between NGF-induced neuritogenesis and expression of heparanase. PC12 cells were harvested after mechanical dislodging, counted using a hemacytometer and then seeded in collagen I-treated 6-well plates (BD Biocoat) at the density of 300 cells / mm^2 in PC12CM. Three days later, cells were treated at day 0 (D0) with 50 ng/mL mouse recombinant 2.5S NGF (Promega) in DMEM completed with 1% heat-inactivated normal horse serum and antibiotics. Cells were collected at D0, D1 and D3 and prepared for determination of heparanase transcript level (n=4 for each day). Western blot analysis of immunoreactive heparanase was performed at D0 and D3. Immunocytochemical detection of heparanase protein was also performed in duplicate wells for each day.

Ex vivo procedures

Tissue preparation for transcript and protein level analysis. To determine the levels of heparanase mRNA and protein, rats were sacrificed following a lethal injection of pentobarbital (250 mg/kg). Cerebral structures were rapidly removed and frozen in liquid nitrogen, and stored at -80°C.

Tissue preparation for histological analysis. To localize and characterize cells expressing heparanase in the brain, rats were deeply anesthetized (lethal intraperitoneal injection of pentobarbital at 250 mg/kg) and transcardially perfused with chilled 4% paraformaldehyde in 0.1M phosphate buffer at flow rates of 15 mL/min for 4 min (5 d) and 30 mL/min for 9 min (3 mo and 12 mo). After cryoprotection in 25% sucrose, brains were frozen in isopentane and stored at -80°C.

Methods

RT-real time PCR. Variations in transcript levels were determined by real time PCR amplification of cDNAs of interest after RT of total mRNAs, as previously detailed (Nadam *et al.* 2007). A synthetic external and non-homologous poly(A) Standard RNA (SmRNA) was used to normalize the RT of mRNAs of biological samples (Morales and Bezin, patent WO2004.092414). Sequences of the different primer pairs used are: BDNF (GenBank X67108) forward 5' AAA TTA CCT GGA TGC CGC AA 3', reverse 5' CGC CAG CCA ATT CTC TTT TT 3' (345 bp), heparanase (GenBank NM_022605) forward 5' CAA TGA TAT TTG CGG GTC TG 3', reverse 5' TGC GTT TTG GAA AGC TGA CT 3' (415 bp) and VEGF (GenBank NM_031836) forward 5' CCT GTG TGC CCC TAA TGC 3', reverse 5' AGG TTT GAT CCG CAT GAT CT 3' (107 bp). All primer pairs were designed using "Primer 3" software (NIH; www.basic.nwu.edu).

Production of a rabbit polyclonal anti-rat heparanase antibody. A polyclonal immuno-affinity purified antibody directed against rat heparanase protein (GenBank NP_072127) has been produced (Covalab, Lyon, France) after immunization of a rabbit with two 13/14-residue peptides located within HS binding domains of the rat heparanase protein (Hulett et al. 1999). The sequences of these peptides are ^{149}YQREKNSTYSRS^{161} and ^{273}RSFLKAGGEVIDS^{284}, both preceded by an additional cystein residue.

Western Blot analysis of immunoreactive heparanase. For each age studied, 50 µg of proteins extracted from the neocortex of each animal were pooled. For each experimental condition performed in PC12 cells, 10 µg of proteins extracted from each triplicate were also pooled together. Equal amounts of pooled proteins (40 µg for tissue samples and 10 µg for PC12 cells) were separated on 12% SDS/PAGE gels and then transferred onto nitrocellulose membranes by standard procedures. The membranes were blocked by incubation in 5% skim milk in TBS buffer containing 0.1% Tween 20 (TBS-T) at room temperature for 1 hour. All washes were performed in TBS buffer. The membranes were successively incubated in avidin and biotin solutions (Avidin Biotin blocking kit; Vector) according to manufacturer's instructions. Then, the membranes were sequentially incubated with a rabbit anti-heparanase polyclonal antibody (Covalab) diluted at 1/100 in TBS-T containing 1% skim

milk (overnight at 4°C), with a biotinylated goat anti-rabbit IgG (AP187B; Chemicon) diluted at 1/10000 in TBS-T containing 1% skim milk (2 hours at room temperature), with avidin biotin peroxydase complex (Vectastain Elite ABC kit; Vector) diluted at 1/1500 in TBS (1 hour at room temperature), and finally reacted with a 3',3-diaminobenzidine (DAB) solution (Vector). After intensive washes in tap-water, membranes were digitalized and analyzed for quantification with an image analysis system (Visilog 6.3; Noesis). For each band, the integrated optical density (OD) and the surface area (S; pixels) were measured. The index of protein level was calculated by multiplying OD with S, and expressed in arbitrary units (A.U.).

Fluorescent immunolabeling of heparanase. Three series of dual-immunolabeling were performed on free-floating sections (40 µm thick) from paraformaldehyde-fixed tissue. Each series consisted of incubating sections with an antibody raised against heparanase together with an antibody raised against either NeuN, or GFAP, or OX-42. In each series, sections from all brain regions and all ages of interest were processed together. Primary antibodies were used at the following dilutions : 1/350 for the rabbit polyclonal anti-heparanase antibody (Covalab), 1/1000 for the mouse monoclonal anti-NeuN antibody (MAB-377; Chemicon), 1/2500 for the mouse monoclonal anti-GFAP antibody (G3893, Sigma) and 1/2000 for the mouse monoclonal anti-OX-42 antibody (CBL1512Z; Chemicon). Primary antibodies were then detected by an Alexa-488-conjugated donkey anti-rabbit IgG antibody (A-21206; Molecular Probes) diluted at 1/2000 and an Alexa-633-conjugated goat anti-mouse IgG antibody (A-21052; Molecular Probes), diluted at 1/1000. Specificity controls of the rabbit anti-heparanase antibody were done by pre-incubating this primary antibody with 10 µM of antigenic peptides used to immunize rabbit. Sections were then mounted on SuperFrost®Plus slides and coverglassed with Prolong Gold Antifade reagent with DAPI (Molecular Probes). Sections of each series of dual-immunolabeling were then analyzed at the same conditions of photomultiplier gain, offset and pinhole aperture using a TCS SP2 confocal microscopy system (Leica), allowing the comparison of fluorescence intensity between regions of interest at all ages examined. Images were finally imported into Adobe Photoshop 8.0.1 (Adobe Systems) for further editing.

Colorimetric immunocytochemical detection of heparanase. After fixation in a 4% paraformaldehyde solution at 4°C, cells were intensively rinsed in PBS, incubated overnight at 4°C in PBS containing

0.5% Triton 100X, and then with the rabbit polyclonal anti-heparanase antibody (see above) diluted at 1/500 for ~ 24h at room temperature. After washes, cells were exposed overnight at 4°C to a biotinylated goat anti-rabbit IgG (AP187B, Chemicon) diluted at 1/2000. After washes, cells were incubated with avidin biotin peroxydase complex (1/500; Vectastain Elite ABC kit, Vector) and reacted with a DAB solution (Vector). Images were captured with a video camera 3CCD (DXC-9300; Sony) coupled to an image analysis system (Visilog 6.3; Noesis).

CD-34 staining and measurement of the surface area occupied by blood vessels. Free-floating sections (40 µm thick) from paraformaldehyde-fixed tissue were incubated for ~ 24h at room temperature with a goat polyclonal antibody raised against CD-34 (Santa Cruz, sc-7045), diluted at 1/500. After washes, sections were exposed overnight at 4°C to a biotinylated donkey anti-goat IgG (705.066.147, Jackson ImmunoResearch) diluted at 1/5000. After washes, sections were incubated with avidin biotin peroxydase complex (1/1000, Vectastain Elite ABC kit, Vector) and reacted with a 3', 3-diaminobenzidine solution (Vector). Images were captured with a video camera 3CCD (DXC-9300, Sony) coupled to an image analysis system (Visilog 6.3, Noesis). The surface area occupied by CD-34+ blood vessels was measured within a 302 340 µm² window using the visilog software.

Fluorescent detection of BrdU+ cells in the hippocampus. Free-floating sections (40 µm thick) were mounted on SuperFrost®Plus slides and air dried. After DNA denaturation for 30 min in 2M HCl at 65°C and neutralization in borate buffer pH 8.5, sections were incubated overnight at 4°C with a rat monoclonal antibody raised against BrdU (OBT-0030; Oxford Biotechnology) diluted at 1/25, and then with an Alexa-488-conjugated donkey anti-rat IgG antibody (A-21208; Molecular Probes) diluted at 1/1000. Sections were then coverglassed with Prolong Gold Antifade reagent (Molecular Probes), and analyzed as described above using a TCS SP2 confocal microscopy system (Leica).

Statistical Analysis

Data are expressed as mean ± SEM of the variables (mRNA level, BrdU+ cell number, blood vessel surface area) and are compared among groups by using one-way ANOVA followed by Fisher's protected Least Significance Differences (LSD) test.

Results

Constitutive expression of brain heparanase in young adult rats

In 3 month-old rats, transcript encoding heparanase was easily detected in all brain structures studied. The hippocampus, the neocortex and the olfactory bulb exhibited similar tissue concentration of heparanase-mRNA, which was greater than that measured in the thalamus and the hypothalamus (Figure 1A).

Heparanase protein was detected by fluorescent immunolabeling in all brain structures analyzed, as illustrated in the pyramidal cell layer of Ammon's horn (Figure 1B) and in the neocortex (Figure 1C). The specificity of the antibody was demonstrated by the lack of fluorescent signal when it was pre-incubated with both antigenic peptides overnight at 4°C before application to brain sections (Figures 1D-E).

Fluorescent dual labeling using antibodies directed against heparanase and neuronal specific marker NeuN evidenced that heparanase expression was restricted to neurons, as illustrated in the hippocampus (Figures 2 A-C) and the neocortex (Figures 2 D-F). It is noteworthy that heparanase was contained in dendritic extensions in these two brain areas (see white arrows in Figures 1 B,C). Immunolabeling of heparanase was neither associated with specific astroglial marker GFAP, nor with microglial specific marker OX-42 (data not shown).

Brain expression of heparanase during postnatal development and ageing

Heparanase transcript levels quantified in the hippocampus (Figure 3A), the neocortex (Figure 3B) and the olfactory bulb (Figure 3C) exhibited highly significant changes throughout postnatal development and ageing ($p<0.001$, ANOVA 1 in each brain area). The hippocampus and the neocortex displayed similar profiles as compared to the olfactory bulb. Indeed, (i) greatest heparanase transcript levels were observed at 2 and 5 days within the hippocampus and the neocortex, while the apparent peak was observed at 1 week in the olfactory bulb, and (ii) a significant increase in heparanase transcript level was noticed between 3 and 12 months in the hippocampus and the neocortex only.

Western blot analysis of immunoreactive heparanase revealed that zymogen and processed active forms of heparanase are specifically detected by the antibody used in the neocortex of 3 month-old rats (Figure 4A). Throughout postnatal development and ageing, the active form (50 kDa) was more abundant than the zymogen form (65 kDa). The level of the zymogen form was at its lowest value at postnatal day 2, gradually increased up to the adult stage (3 months) and remained stable during ageing. By contrast, the active form was the most abundant at postnatal day 2 and attained its stabilized level by the second postnatal week. The ratio “active form / zymogen form” thus reached its greatest value at postnatal day 2 (Figure 4B).

Immunohistochemical detection of heparanase performed at postnatal day 5 evidenced a dense punctuate signal in the *stratum radiatum* of area CA1 (Figure 4C). This punctuate signal may reflect the presence of the enzyme in numerous neuronal varicosities, as supported by the labeling observed within neuronal processes in the neocortex (see white arrow, Figure 4D). The punctuate signal increased in density within the neuropile throughout development and ageing in the neocortex, as illustrated at 12 months (Figure 4F).

Heparanase could not be detected within granule cell bodies in the dentate gyrus (data not shown), pyramidal neurons of Ammon’s horn (Figure 4C), and neocortical neurons (Figure 4D) at postnatal day 5. By contrast, later during ageing, heparanase was unequivocally detected in cell bodies of pyramidal neurons of Ammon’s horn (Figures 1C and 4E) and neocortical neurons (Figures 1C and 4F) by 3 months, and in granule cell bodies of dentate gyrus by 12 months only (data not shown).

Increased heparanase expression during NGF-induced neuronal differentiation in PC12 cells

Heparanase transcript was constitutively expressed by exponentially growing PC12 cells, and transcript level was not affected by cell density (data not shown). During NGF-induced neuritic extension, we observed that heparanase transcript level gradually increased, reaching + 413% and + 1861% after 1 day and 3 days of NGF-treatment, respectively, as compared to controls (day 0) (Figure 5A). Increased heparanase mRNA levels were accompanied by the detection of the protein within neuritic extension (see black arrow, Figure 5B). The zymogen form of heparanase (65 kDa) was detected at comparable levels in growing PC12 cells (D0) and 3 days (D3) after NGF-induced

neuronal differentiation, while the active form of the enzyme was more abundantly found in NGF-treated cells (Figure 5C).

Hypoxia-induced angiogenesis correlates with enhanced heparanase transcript level in the hippocampus

A single transient severe hypoxic episode was not sufficient to elicit detectable angiogenesis, as measured by the surface area occupied by CD34-immunostained endothelial cells (Figure 6A), despite a significant increase in VEGF mRNA level (+ 218%, Figure 6B). Heparanase gene expression remained unchanged immediately (Figure 6B), 1, 2 and 8 days (data not shown) after this single hypoxic exposure. By contrast, heparanase mRNA level was greatly enhanced following three severe hypoxic exposures, the apparent peak being observed immediately after the last hypoxic exposure (+ 262%, Figure 6B), control levels being recovered 8 days later (data not shown). The apparent peak of VEGF transcript level (+ 353%, Figure 6B) was measured immediately after the last hypoxic exposure, control levels being recovered 1 day later (data not shown). Following three severe hypoxic exposures, we measured a significant increase in the surface area occupied by CD34-immunostained endothelial cells (+ 36%, Figure 6A).

Environmental enrichment fails to up-regulate heparanase transcript level

Environmental enrichment is a situation of increased brain plasticity (Nithianantharajah & Hannan 2006). Here we evidence in the hippocampus that rats housed in an enriched environment had an increased VEGF transcript level (Figure 7B), as previously reported (Cao *et al.* 2004), and a greater number of BrdU-incorporating cells in the dentate gyrus (Figure 7A), indicating that neurogenesis was enhanced (Stranahan et al. 2006, van Praag et al. 2000). Despite the tissue remodeling accompanying increased neurogenesis, heparanase transcript level remained stable (Figure 7B).

Discussion

This study provides evidence that heparanase is mainly expressed by neurons in the brain throughout lifespan. We show that heparanase transcript level is increased in conditions associated with intensive structural plasticity, such as occurs during early postnatal maturation or during acclimatization to repeated hypoxic challenges.

In agreement with a prior study performed in the brain of adult blind mole rats (Nasser et al. 2005), we detected heparanase transcript and protein in the forebrain of mature Sprague-Dawley rats. Tissue distribution analysis of heparanase transcript in blind mole rats revealed less abundant levels in the brain than in the kidney and the liver (Nasser et al. 2005). This analysis was performed using whole brain extracts and could not reveal whether brain expression of heparanase is greater in areas known to be the place of intensive structural plasticity at the adult age. The neocortex displays extraordinary dendritic plasticity in response to environmental changes (Hickmott & Ethell 2006), and both the hippocampus and the olfactory bulb undergo intensive morphological changes associated with neurogenesis (Ming & Song 2005). Here we report for the first time that these three brain areas expressed the highest levels of heparanase transcript compared to the other brain areas examined, which may correlate with their capacity to undergo physiological structural remodeling.

While heparanase transcript has been detected both in neurons and astrocytes in the spinal cord of adult rats (Zhang et al. 2006), our study provides evidence that heparanase protein is expressed above detectable levels within the rat forebrain by neurons exclusively. Heparanase is synthesized as a latent 65 kDa precursor and undergoes intracellular lysosomal processing yielding an active heterodimer enzyme composed of 50 and 8 kDa polypeptides (Fairbanks et al. 1999, Levy-Adam et al. 2003, McKenzie et al. 2003, Nardella et al. 2004). In our study, the western blot analysis of immunoreactive heparanase indicates that the predominant form detected is the active 50 kDa form. This result indicates that the major form of the heparanase detected in neurons is the active form of the enzyme, suggesting that lysosomal maturation of the latent 65 kDa pro-enzyme can occur in neurons. We were not able to detect heparanase protein *in vivo* within astrocytes, contrasting with results

obtained *in vitro* by others (Marchetti et al. 2000) and by us (unpublished data), using primary cultures of astrocytes. Heparanase expression that we demonstrate here to be restricted to neurons under basal conditions may extend to astrocytes under pathophysiological conditions, as suggested *in vitro* during invasion of melanoma cells within the brain parenchyma (Marchetti et al. 2000). Recent studies revealed that heparanase protein can be found both in the cytoplasm and the nucleus of differentiating cells (Kobayashi *et al.* 2006, Nobuhisa *et al.* 2007). We detected heparanase protein only in the cytoplasm of neurons, which is in agreement with studies which reported high levels of heparanase protein in the cytoplasm of peripheral neurons in human normal tissues (Dong *et al.* 2000). It is noteworthy that we detected heparanase protein in dendrites of pyramidal neurons in area CA1, which exhibit cell-surface HSPGs (Yamaguchi 2001) essential for the morphological maturation of spines (Ethell *et al.* 2001), suggesting that co-localization of heparanase and HSPGs in neuronal processes may contribute to precisely control HSPG turn-over.

Prior studies have suggested that heparanase plays a critical role in the developing nervous system (Goldshmidt et al. 2001) and during neural cellular differentiation (Moretti *et al.* 2006), a hypothesis strengthened by our observation that (i) heparanase protein is present in numerous varicosities within the forebrain during the early postnatal period, and (ii) heparanase gene expression is increased during neuronal differentiation of PC12 cells. Both zymogen and active forms of heparanase have been shown to play biological functions (Goldshmidt *et al.* 2003, Sotnikov *et al.* 2004). Our observation that the 50 kDa form level is considerably high at early stages of postnatal development, as well as during NGF-induced neuritogenesis of PC12 cells, suggests that the major form of heparanase which is involved during development of the nervous system is the processed active heterodimer. Processes of neuronal death, neuronal differentiation (with dendritic growth and synaptogenesis) and axonal pathfinding that occur throughout the developmental period (Bayer *et al.* 1993, Luhmann *et al.* 2003) are known to be regulated by HSPGs (Perrimon & Bernfield 2000, Yamaguchi 2001). These cellular events require morphogen molecules including members of the Hedgehog, Wingless and fibroblast growth factor families (Bovolenta & Marti 2005, Reuss & von Bohlen und Halbach 2003), the signaling pathways of which are modified after binding to

extracellular HS chains (Lin 2004, Lin *et al.* 1999, Ornitz & Leder 1992, Rapraeger *et al.* 1991, Yayon *et al.* 1991). The presence of HS chains largely depends on both HS biosynthetic and degrading enzymes. HS synthesis is governed by (i) *Ext* genes, a family of glycosyltransferases that catalyse polymerization of alternating N-acetylglucosamine and glucuronic acid disaccharides that form the core of HS chains (Duncan *et al.* 2001), and (ii) epimerases and sulfotransferases, that support sequential modifications of HS (Perrimon & Bernfield 2000). The highest levels of transcripts encoding EXT-1, EXT-2 and some members of sulfotransferases have been measured in the forebrain of mice during the first postnatal week (Inatani & Yamaguchi 2003, Yabe *et al.* 2005). Here, by demonstrating that apparent peaks of transcript and active form of heparanase occur during the first postnatal week also in the forebrain, we can hypothesize that degradation of HS chains is increased. Altogether, these results suggest that the turn-over of HS chains is enhanced during the early postnatal period, which may be critical in the modulation of morphogen signaling involved in the structural plasticity of the developing brain.

The observation that brain heparanase transcript level correlated with tissue plasticity throughout postnatal development encouraged us to investigate whether heparanase gene expression could be reactivated in adult rats under physiological conditions associated with intensive structural changes. We thus investigated whether physiological responses to severe environmental challenges, such as hypoxia, could imply an up-regulation of brain heparanase gene expression. Indeed, data obtained in hypoxia-tolerant blind mole rats suggest that high level of heparanase molecules may serve some species to adapt to severe hypoxic environments by facilitating tissue vascularization (Nasser et al. 2005). Hypoxia-induced brain angiogenesis is considered to be regulated by similar mechanisms as pathological angiogenesis induced by tumors, involving increased expression of VEGF and heparanase (Bernaudin *et al.* 2002, Chavez *et al.* 2000, Greenberg & Jin 2005, Plate 1999, Plate *et al.* 1992). Here we show for the first time that the repetition of severe hypoxia episodes triggers a robust induction of both heparanase and VEGF mRNA in the adult rat hippocampus, associated with an increased vascularity. However, the upregulation of VEGF gene expression alone observed after a single episode of severe hypoxia is not a sufficient stimulus to promote enhanced vascularity. We thus

suggest that the coordinate upregulation of heparanase and VEGF gene expression is the ideal condition to promote angiogenesis. In addition, the recent demonstration that upregulated heparanase level increases VEGF gene expression in tumor-derived cell lines (Zetser *et al.* 2006) provides a potential mechanisms that may explain the overinduction of VEGF transcript level observed after three hypoxic episodes in the hippocampus.

Heparanase gene expression remained stable in the hippocampus of adult rats housed in an enriched environment, despite a ~2-fold increase in the number of newly-generated neurons. This result suggests that basal level and/or specific activity of neuronal heparanase in the hippocampus at adulthood is sufficient to support differentiation and migration of newborn neurons and pathfinding of their axonal and dendritic processes. Altogether, our results suggest that upregulation of heparanase gene expression in the adult rat brain may support specific tissue remodeling, such as the increased vascularity occurring after repeated hypoxia exposures or during tumor angiogenesis. Finally, the evidence that neurons is a source of heparanase in the brain parenchyma highlights that therapeutic approaches aimed at inhibiting its enzymatic activity in tumor cells may affect the potential role played by heparanase in brain homeostasis. However, in the case of brain metastasis, inhibition of neuronal heparanase activity may be beneficial to counteract brain colonization by tumor cells.

Acknowledgements

We thank Pr. Jean-Jacques Madjar and Dr. Caroline Anselme for their efficient assistance in western blot analysis. We also thank Denis Ressnikoff and Yves Tourneur from the Centre Commun de Quantimétrie of the Université Lyon 1 for their technical assistance in confocal microscopy studies. This research was supported by grants from the Centre National de la Recherche Scientifique and the Université Claude Bernard Lyon 1. P. Sanchez is a PhD Student fellow from the Délégation Générale pour l'Armement, Ministère français de la défense.

References

Bayer, S. A., Altman, J., Russo, R. J. and Zhang, X. (1993) Timetables of neurogenesis in the human brain based on experimentally determined patterns in the rat. *Neurotoxicology,* **14,** 83-144.

Bernaudin, M., Nedelec, A. S., Divoux, D., MacKenzie, E. T., Petit, E. and Schumann-Bard, P. (2002) Normobaric hypoxia induces tolerance to focal permanent cerebral ischemia in association with an increased expression of hypoxia-inducible factor-1 and its target genes, erythropoietin and VEGF, in the adult mouse brain. *J Cereb Blood Flow Metab,* **22,** 393-403.

Bovolenta, P. and Marti, E. (2005) Introduction: unexpected roles for morphogens in the development and regeneration of the CNS. *J Neurobiol,* **64,** 321-323.

Cao, L., Jiao, X., Zuzga, D. S., Liu, Y., Fong, D. M., Young, D. and During, M. J. (2004) VEGF links hippocampal activity with neurogenesis, learning and memory. *Nat Genet,* **36,** 827-835.

Chavez, J. C., Agani, F., Pichiule, P. and LaManna, J. C. (2000) Expression of hypoxia-inducible factor-1alpha in the brain of rats during chronic hypoxia. *J Appl Physiol,* **89,** 1937-1942.

Deepa, S. S., Yamada, S., Zako, M., Goldberger, O. and Sugahara, K. (2004) Chondroitin sulfate chains on syndecan-1 and syndecan-4 from normal murine mammary gland epithelial cells are structurally and functionally distinct and cooperate with heparan sulfate chains to bind growth factors. A novel function to control binding of midkine, pleiotrophin, and basic fibroblast growth factor. *J Biol Chem,* **279,** 37368-37376.

Dong, J., Kukula, A. K., Toyoshima, M. and Nakajima, M. (2000) Genomic organization and chromosome localization of the newly identified human heparanase gene. *Gene,* **253,** 171-178.

Duncan, G., McCormick, C. and Tufaro, F. (2001) The link between heparan sulfate and hereditary bone disease: finding a function for the EXT family of putative tumor suppressor proteins. *J Clin Invest,* **108,** 511-516.

Esko, J. D. and Selleck, S. B. (2002) Order out of chaos: assembly of ligand binding sites in heparan sulfate. *Annu Rev Biochem,* **71,** 435-471.

Ethell, I. M., Irie, F., Kalo, M. S., Couchman, J. R., Pasquale, E. B. and Yamaguchi, Y. (2001) EphB/syndecan-2 signaling in dendritic spine morphogenesis. *Neuron,* **31,** 1001-1013.

Fairbanks, M. B., Mildner, A. M., Leone, J. W. et al. (1999) Processing of the human heparanase precursor and evidence that the active enzyme is a heterodimer. *J Biol Chem,* **274,** 29587-29590.

Gallagher, J. T. (2001) Heparan sulfate: growth control with a restricted sequence menu. *J Clin Invest,* **108,** 357-361.

Gingis-Velitski, S., Zetser, A., Kaplan, V. et al. (2004) Heparanase uptake is mediated by cell membrane heparan sulfate proteoglycans. *J Biol Chem,* **279,** 44084-44092.

Goldshmidt, O., Zcharia, E., Aingorn, H., Guatta-Rangini, Z., Atzmon, R., Michal, I., Pecker, I., Mitrani, E. and Vlodavsky, I. (2001) Expression pattern and secretion of human and chicken heparanase are determined by their signal peptide sequence. *J Biol Chem,* **276,** 29178-29187.

Goldshmidt, O., Zcharia, E., Cohen, M., Aingorn, H., Cohen, I., Nadav, L., Katz, B. Z., Geiger, B. and Vlodavsky, I. (2003) Heparanase mediates cell adhesion independent of its enzymatic activity. *Faseb J,* **17,** 1015-1025.

Greenberg, D. A. and Jin, K. (2005) From angiogenesis to neuropathology. *Nature,* **438,** 954-959.

Hickmott, P. W. and Ethell, I. M. (2006) Dendritic plasticity in the adult neocortex. *Neuroscientist,* **12,** 16-28.

Hulett, M. D., Freeman, C., Hamdorf, B. J., Baker, R. T., Harris, M. J. and Parish, C. R. (1999) Cloning of mammalian heparanase, an important enzyme in tumor invasion and metastasis. *Nat Med,* **5,** 803-809.

Inatani, M. and Yamaguchi, Y. (2003) Gene expression of EXT1 and EXT2 during mouse brain development. *Brain Res Dev Brain Res,* **141,** 129-136.

Ishai-Michaeli, R., Eldor, A. and Vlodavsky, I. (1990) Heparanase activity expressed by platelets, neutrophils, and lymphoma cells releases active fibroblast growth factor from extracellular matrix. *Cell Regul,* **1,** 833-842.

Kobayashi, M., Naomoto, Y., Nobuhisa, T. et al. (2006) Heparanase regulates esophageal keratinocyte differentiation through nuclear translocation and heparan sulfate cleavage. *Differentiation,* **74,** 235-243.

Kussie, P. H., Hulmes, J. D., Ludwig, D. L., Patel, S., Navarro, E. C., Seddon, A. P., Giorgio, N. A. and Bohlen, P. (1999) Cloning and functional expression of a human heparanase gene. *Biochem Biophys Res Commun,* **261,** 183-187.

Lander, A. D. (1993) Proteoglycans in the nervous system. *Curr Opin Neurobiol,* **3,** 716-723.

Levy-Adam, F., Miao, H. Q., Heinrikson, R. L., Vlodavsky, I. and Ilan, N. (2003) Heterodimer formation is essential for heparanase enzymatic activity. *Biochem Biophys Res Commun,* **308,** 885-891.

Lin, X. (2004) Functions of heparan sulfate proteoglycans in cell signaling during development. *Development,* **131,** 6009-6021.

Lin, X., Buff, E. M., Perrimon, N. and Michelson, A. M. (1999) Heparan sulfate proteoglycans are essential for FGF receptor signaling during Drosophila embryonic development. *Development,* **126,** 3715-3723.

Lindahl, U., Kusche-Gullberg, M. and Kjellen, L. (1998) Regulated diversity of heparan sulfate. *J Biol Chem,* **273,** 24979-24982.

Lortat-Jacob, H., Grosdidier, A. and Imberty, A. (2002) Structural diversity of heparan sulfate binding domains in chemokines. *Proc Natl Acad Sci U S A,* **99,** 1229-1234.

Luhmann, H. J., Hanganu, I. and Kilb, W. (2003) Cellular physiology of the neonatal rat cerebral cortex. *Brain Res Bull,* **60,** 345-353.

Lyon, M. and Gallagher, J. T. (1998) Bio-specific sequences and domains in heparan sulphate and the regulation of cell growth and adhesion. *Matrix Biol,* **17,** 485-493.

Marchetti, D., Li, J. and Shen, R. (2000) Astrocytes contribute to the brain-metastatic specificity of melanoma cells by producing heparanase. *Cancer Res,* **60,** 4767-4770.

Marchetti, D. and Nicolson, G. L. (2001) Human heparanase: a molecular determinant of brain metastasis. *Adv Enzyme Regul,* **41,** 343-359.

Margolis, R. K. and Margolis, R. U. (1993) Nervous tissue proteoglycans. *Experientia,* **49,** 429-446.

McKenzie, E., Young, K., Hircock, M. et al. (2003) Biochemical characterization of the active heterodimer form of human heparanase (Hpa1) protein expressed in insect cells. *Biochem J,* **373,** 423-435.

Miao, H. Q., Navarro, E., Patel, S. et al. (2002) Cloning, expression, and purification of mouse heparanase. *Protein Expr Purif,* **26,** 425-431.

Ming, G. L. and Song, H. (2005) Adult neurogenesis in the mammalian central nervous system. *Annu Rev Neurosci,* **28,** 223-250.

Miyamoto, O., Sumitani, K., Takahashi, M., Hirakawa, H., Kusakabe, T., Hayashida, Y. and Itano, T. (2005) Vascular changes in the rat brain during chronic hypoxia in the presence and absence of hypercapnia. *Acta Med Okayama,* **59,** 135-143.

Moretti, M., Sinnappah-Kang, N. D., Toller, M., Curcio, F. and Marchetti, D. (2006) HPSE-1 expression and functionality in differentiating neural cells. *J Neurosci Res,* **83,** 694-701.

Nadam, J., Navarro, F., Sanchez, P. et al. (2007) Neuroprotective effects of erythropoietin in the rat hippocampus after pilocarpine-induced status epilepticus. *Neurobiol Dis,* **25,** 412-426.

Nakajima, M., Irimura, T. and Nicolson, G. L. (1988) Heparanases and tumor metastasis. *J Cell Biochem,* **36,** 157-167.

Nardella, C., Lahm, A., Pallaoro, M., Brunetti, M., Vannini, A. and Steinkuhler, C. (2004) Mechanism of activation of human heparanase investigated by protein engineering. *Biochemistry,* **43,** 1862-1873.

Nasser, N. J., Nevo, E., Shafat, I., Ilan, N., Vlodavsky, I. and Avivi, A. (2005) Adaptive evolution of heparanase in hypoxia-tolerant Spalax: gene cloning and identification of a unique splice variant. *Proc Natl Acad Sci U S A,* **102,** 15161-15166.

Nithianantharajah, J. and Hannan, A. J. (2006) Enriched environments, experience-dependent plasticity and disorders of the nervous system. *Nat Rev Neurosci,* **7,** 697-709.

Nobuhisa, T., Naomoto, Y., Okawa, T. et al. (2007) Translocation of heparanase into nucleus results in cell differentiation. *Cancer Sci,* **98,** 535-540.

Okada, Y., Yamada, S., Toyoshima, M., Dong, J., Nakajima, M. and Sugahara, K. (2002) Structural recognition by recombinant human heparanase that plays critical roles in tumor metastasis. Hierarchical sulfate groups with different effects and the essential target disulfated trisaccharide sequence. *J Biol Chem,* **277,** 42488-42495.

Ornitz, D. M. and Leder, P. (1992) Ligand specificity and heparin dependence of fibroblast growth factor receptors 1 and 3. *J Biol Chem,* **267,** 16305-16311.

Parish, C. R. (2006) The role of heparan sulphate in inflammation. *Nat Rev Immunol,* **6,** 633-643.

Parish, C. R., Coombe, D. R., Jakobsen, K. B., Bennett, F. A. and Underwood, P. A. (1987) Evidence that sulphated polysaccharides inhibit tumour metastasis by blocking tumour-cell-derived heparanases. *Int J Cancer,* **40,** 511-518.

Parish, C. R., Freeman, C. and Hulett, M. D. (2001) Heparanase: a key enzyme involved in cell invasion. *Biochim Biophys Acta,* **1471,** M99-108.

Patt, S., Sampaolo, S., Theallier-Janko, A., Tschairkin, I. and Cervos-Navarro, J. (1997) Cerebral angiogenesis triggered by severe chronic hypoxia displays regional differences. *J Cereb Blood Flow Metab,* **17,** 801-806.

Perrimon, N. and Bernfield, M. (2000) Specificities of heparan sulphate proteoglycans in developmental processes. *Nature,* **404,** 725-728.

Pikas, D. S., Li, J. P., Vlodavsky, I. and Lindahl, U. (1998) Substrate specificity of heparanases from human hepatoma and platelets. *J Biol Chem,* **273,** 18770-18777.

Plate, K. H. (1999) Mechanisms of angiogenesis in the brain. *J Neuropathol Exp Neurol,* **58,** 313-320.

Plate, K. H., Breier, G., Weich, H. A. and Risau, W. (1992) Vascular endothelial growth factor is a potential tumour angiogenesis factor in human gliomas in vivo. *Nature,* **359,** 845-848.

Rapraeger, A. C. (1995) In the clutches of proteoglycans: how does heparan sulfate regulate FGF binding? *Chem Biol,* **2,** 645-649.

Rapraeger, A. C., Krufka, A. and Olwin, B. B. (1991) Requirement of heparan sulfate for bFGF-mediated fibroblast growth and myoblast differentiation. *Science,* **252,** 1705-1708.

Reuss, B. and von Bohlen und Halbach, O. (2003) Fibroblast growth factors and their receptors in the central nervous system. *Cell Tissue Res,* **313,** 139-157.

Sotnikov, I., Hershkoviz, R., Grabovsky, V., Ilan, N., Cahalon, L., Vlodavsky, I., Alon, R. and Lider, O. (2004) Enzymatically quiescent heparanase augments T cell interactions with VCAM-1 and extracellular matrix components under versatile dynamic contexts. *J Immunol,* **172,** 5185-5193.

Stranahan, A. M., Khalil, D. and Gould, E. (2006) Social isolation delays the positive effects of running on adult neurogenesis. *Nat Neurosci,* **9,** 526-533.

Taipale, J. and Keski-Oja, J. (1997) Growth factors in the extracellular matrix. *Faseb J,* **11,** 51-59.

Thunberg, L., Backstrom, G., Wasteson, A., Robinson, H. C., Ogren, S. and Lindahl, U. (1982) Enzymatic depolymerization of heparin-related polysaccharides. Substrate specificities of mouse mastocytoma and human platelet endo-beta-D-glucuronidases. *J Biol Chem,* **257,** 10278-10282.

Toyoshima, M. and Nakajima, M. (1999) Human heparanase. Purification, characterization, cloning, and expression. *J Biol Chem,* **274,** 24153-24160.

Turnbull, J., Powell, A. and Guimond, S. (2001) Heparan sulfate: decoding a dynamic multifunctional cell regulator. *Trends Cell Biol,* **11,** 75-82.

van Praag, H., Kempermann, G. and Gage, F. H. (2000) Neural consequences of environmental enrichment. *Nat Rev Neurosci,* **1,** 191-198.

Vaquero, J., Zurita, M., Coca, S., Oya, S. and Morales, C. (2000) Prognostic significance of clinical and angiogenesis-related factors in low-grade oligodendrogliomas. *Surg Neurol,* **54,** 229-234; discussion 234.

Vlodavsky, I., Friedmann, Y., Elkin, M. et al. (1999) Mammalian heparanase: gene cloning, expression and function in tumor progression and metastasis. *Nat Med,* **5,** 793-802.

Yabe, T., Hata, T., He, J. and Maeda, N. (2005) Developmental and regional expression of heparan sulfate sulfotransferase genes in the mouse brain. *Glycobiology,* **15,** 982-993.

Yamaguchi, Y. (2001) Heparan sulfate proteoglycans in the nervous system: their diverse roles in neurogenesis, axon guidance, and synaptogenesis. *Semin Cell Dev Biol,* **12,** 99-106.

Yayon, A., Klagsbrun, M., Esko, J. D., Leder, P. and Ornitz, D. M. (1991) Cell surface, heparin-like molecules are required for binding of basic fibroblast growth factor to its high affinity receptor. *Cell,* **64,** 841-848.

Young, P. E., Baumhueter, S. and Lasky, L. A. (1995) The sialomucin CD34 is expressed on hematopoietic cells and blood vessels during murine development. *Blood,* **85,** 96-105.

Zetser, A., Bashenko, Y., Edovitsky, E., Levy-Adam, F., Vlodavsky, I. and Ilan, N. (2006) Heparanase induces vascular endothelial growth factor expression: correlation with p38 phosphorylation levels and Src activation. *Cancer Res,* **66,** 1455-1463.

Zhang, Y., Yeung, M. N., Liu, J., Chau, C. H., Chan, Y. S. and Shum, D. K. (2006) Mapping heparanase expression in the spinal cord of adult rats. *J Comp Neurol,* **494,** 345-357.

Figure Legends

Figure 1: Heparanase gene expression in different brain regions of adult rats. (A) Expression profile of heparanase transcript level in the hippocampus, the neocortex, the olfactory bulb, the dorsal part of thalamus and the hypothalamus. Results are expressed as the mean ± SEM number of cDNA copies quantified by real time PCR following RT of mRNAs contained in 500 ng of total RNAs. ** $p<0.01$, *** $p<0.001$ (Fisher LSD test following one-way ANOVA) as compared to the averaged level of heparanase transcript (5168 ± 373 copies) calculated in the hippocampus, the neocortex and the olfactory bulb. †† $p<0.01$ (Fisher LSD test following one-way ANOVA). (B-C) Distribution of heparanase protein in area CA1 of the hippocampus (B) and the neocortex (C). Note the labeling of neuronal processes in these two brain regions (B, C white arrows). (D-E) The specificity of the antibody raised against heparanase is verified by the complete disappearance of the green fluorescent signal normally obtained in brain sections, as illustrated in area CA1 of the hippocampus (D), after pre-incubation of the antibody with both antigenic peptides (E). The blue fluorescent signal corresponds to DAPI nuclear staining. Scale bar: B, 50 µm; D 10 µm. Abbreviations: Hi, hippocampus; NCx, neocortex; OB, olfactory bulb; Thal D, dorsal part of thalamus; Hyp, hypothalamus; so, stratum oriens; sp, stratum pyramidale; sr, stratum radiatum.

Figure 2: Phenotypic characterization of heparanase expressing cells in area CA1 of the hippocampus (A-C) and the neocortex (D-F) in 3 month-old rats. Dual fluorescent labelings indicate that heparanase (A,D; green) is strictly expressed by neurons (B,E; red), using NeuN as a specific neuronal marker. Note the labeling in neuronal processes in area CA1 (A) and in the neocortex (D) (white arrows). Scale bars: A, 25 µm; D, 10 µm. Abbreviations: HEP, heparanase; NCx, neocortex.

Figure 3: Expression profile of heparanase transcript in the hippocampus, the neocortex and the olfactory bulb throughout postnatal development and ageing. (A-C) Numbers of cDNA copies are obtained by real time PCR quantification following RT of mRNAs contained in 500 ng of total RNAs. Results are expressed in percent ± SEM of the value determined in 3 month-old rats. * $p<0.05$, **

p<0.01, *** p<0.001 (Fisher LSD test following one-way ANOVA) as compared to 3 month-old rats. †† p<0.01, ††† p<0.001 (Fisher LSD test following one-way ANOVA) as compared to the preceding age. Abbreviations: d, day; w, week; mo, month.

Figure 4: Heparanase protein expression and distribution in the developing and ageing rat brain. (A) Both zymogen and active forms of heparanase are specifically detected in the neocortex of a 3 month-old rat on a western blot using the antibody developed and used throughout the study. (B) Measurement of zymogen and active forms of immunoreactive heparanase present in the neocortex throughout postnatal development and ageing. (C-F) Distribution of heparanase protein in area CA1 of the hippocampus (C, E) and in the neocortex (D, F) at day 5 (C, D) and at 12 months (E, F). Note the presence of the protein in neuronal processes in area CA1 (E, white arrows) and the neocortex (D, F white arrows). Scale bar: A, 25 µm. Abbreviations: d, day; mo, month; DG, dentate gyrus; so, stratum oriens; sp, stratum pyramidale; sr, stratum radiatum; NCx, neocortex; w, week.

Figure 5: Increased expression of heparanase correlates with neuritogenesis during NGF-induced neuronal differentiation of PC12 cells. (A) Expression profile of heparanase transcript after NGF-treatment (50 ng/mL) in PC12 cells. Number of cDNA copies was measured by real time PCR quantification following RT of mRNAs contained in 500 ng of total RNAs. Results obtained after 1 day (D1) and 3 days (D3) of NGF treatment are expressed in percent ± SEM of the value determined at D0 (control PC12 cells, without NGF treatment). * p<0.05, ** p<0.01 (Fisher LSD test following one-way ANOVA) as compared to D0. (B) Immunolabeling of heparanase in PC12 cells at D0, D1 and D3. Note the detection of heparanase in neuritic extensions of neuron-like PC12 cells (black arrows). (C) Western blot analysis of immunoreactive heparanase in undifferentiated PC12 cells (D0) and in neuron-like differentiated PC12 cells (D3). Scale bar: 50 µm. Abbreviations: NGF, Nerve Growth Factor; HEP, heparanase; D, day.

Figure 6: Hypoxia-induced neovascularization correlates with increased expression of heparanase transcript in the adult rat hippocampus. (A) Brain capillaries could be observed after CD-34

immunostaining. The cell surface occupied by brain capillaries has been measured as illustrated in the enlarged boxes, after delineation of the immunostained capillaries, in control rats (CTRL), or in rats exposed to 1 (H1) or 3 (H3) session(s) of transient hypoxia (8% 0_2 for 6 hours). Hypoxia protocols are detailed in methods. Results are expressed in percent ± SEM of the value determined in controls (0.124 ± 0.011 µm²/µm²). * p<0.05, (Fisher LSD test following one-way ANOVA) as compared to controls. (B) Expression profiles of VEGF and heparanase transcripts after transient hypoxia. Numbers of cDNA copies was obtained by real time PCR quantification following RT of mRNAs contained in 500 ng of total RNAs, and results are expressed in percent ± SEM of the value determined in controls. * p<0.05, *** p<0.001 (Fisher LSD test following one-way ANOVA) as compared to controls. †† p<0.01, ††† p<0.001 (Fisher LSD test following one-way ANOVA) as compared to H1 group. Scale bar: 100 µm. Abbreviations: CTRL, control; VEGF, Vascular Endothelial Growth Factor.

Figure 7: Physiological stimulation of hippocampal neurogenesis in adult rats housed in enriched environment does not require upregulation of heparanase gene expression. (A) BrdU-incorporating cells were counted in the granule cell layer and subgranular zone of the dentate gyrus of the hippocampal formation in rats sacrificed 10 days after the first of 5 injections of BrdU (50 mg/kg), as detailed in the method section. Results obtained in rats housed in an enriched environment (EE) are expressed in percent ± SEM of the value measured in rats housed in a standard environment (SE). (B) Expression profile of VEGF and heparanase transcripts in the hippocampus according to housing conditions. Numbers of cDNA copies are obtained by real time PCR quantification following calibrated RT of mRNAs contained in 500 ng of total RNAs. Results are expressed in percent ± SEM of the value determined in SE rats. *** p<0.001 (Fisher LSD test following one-way ANOVA) as compared to SE rats. Abbreviations: SE, standard environment; EE, enriched environment ; HEP, heparanase ; VEGF, Vascular Endothelial Growth Factor. Scale bar: A, 50 µm.

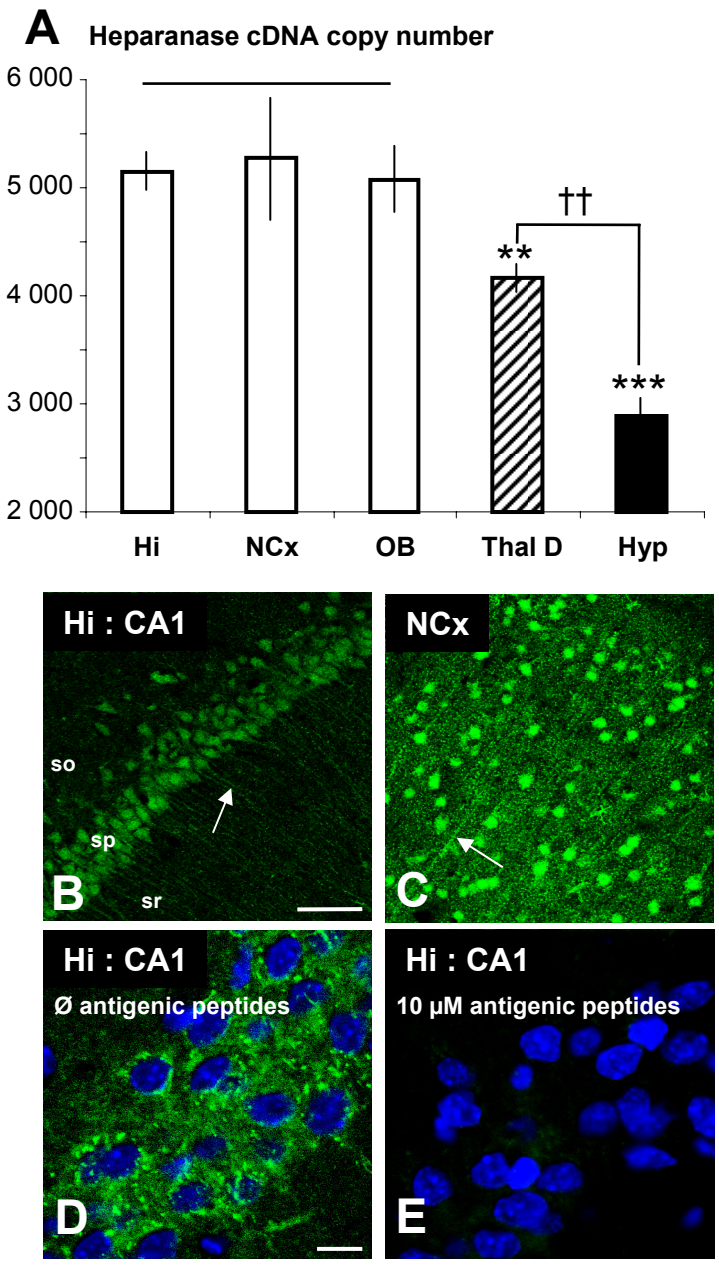
A
Heparanase cDNA copy number
6 000
5 000
4 000
3 000
2 000
Hi
NCx
OB
Thal D
Hyp
**
***
††
Hi : CA1
so
sp
sr
B
NCx
C
Hi : CA1
Ø antigenic peptides
D
Hi : CA1
10 µM antigenic peptides
E

Figure 1

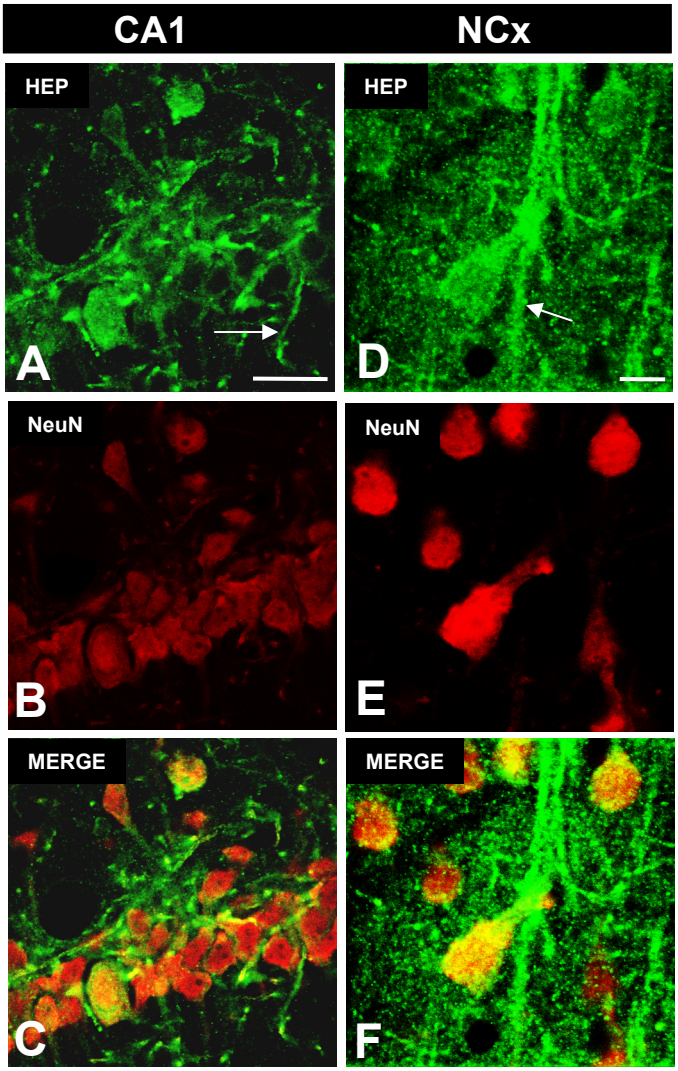

Figure 2

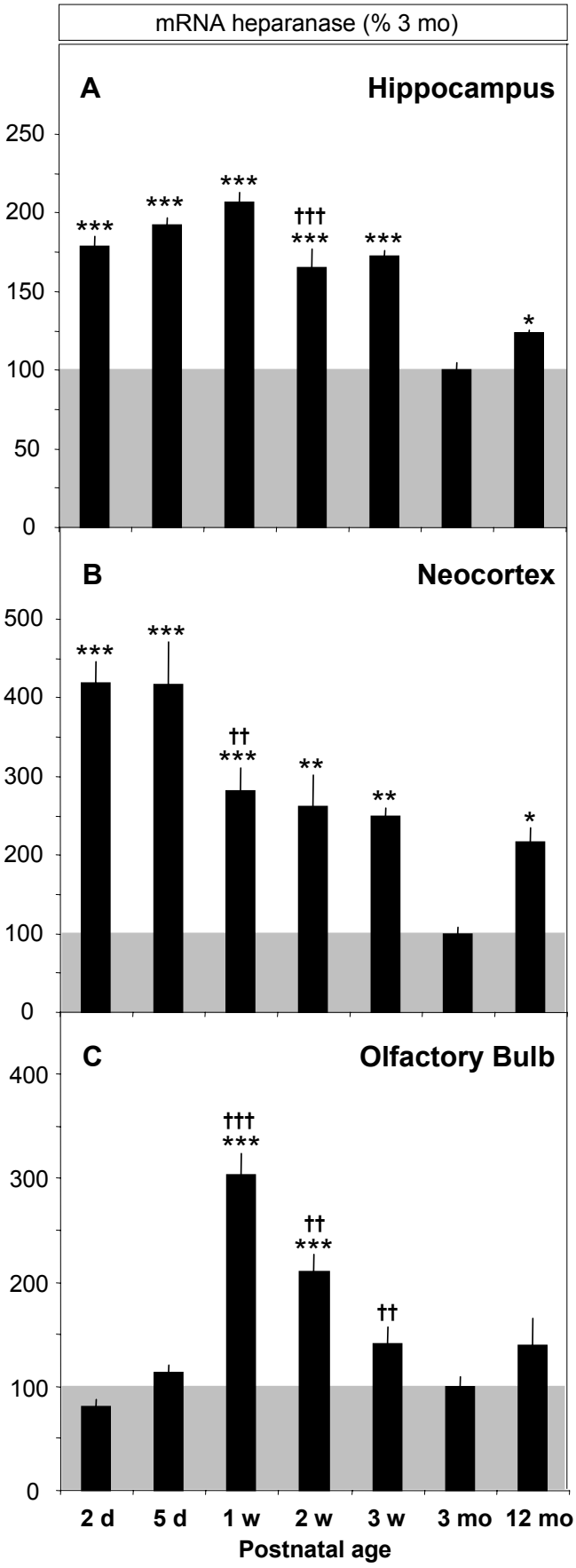
mRNA heparanase (% 3 mo)
A
Hippocampus
250
200
150
100
50
0
***
***
***
†††
***
***
*
B
Neocortex
500
400
300
200
100
0
***
***
††
***
**
**
*
C
Olfactory Bulb
400
300
200
100
0
†††
***
††
***
††
2 d
5 d
1 w
2 w
3 w
3 mo
12 mo
Postnatal age

Figure 3

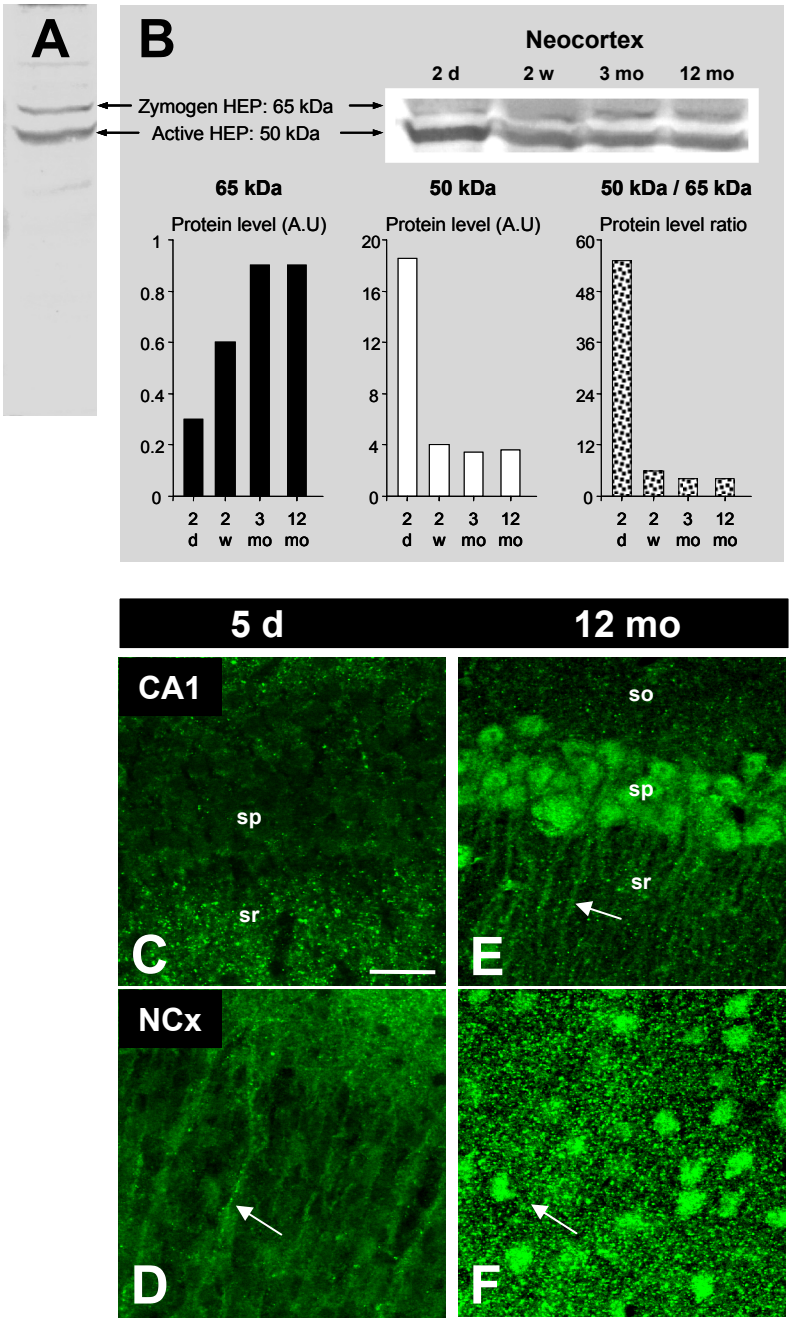
A
B
Neocortex
2 d
2 w
3 mo
12 mo
Zymogen HEP: 65 kDa
Active HEP: 50 kDa
65 kDa
50 kDa
50 kDa / 65 kDa
Protein level (A.U)
Protein level (A.U)
Protein level ratio
1
0.8
0.6
0.4
0.2
0
20
16
12
8
4
0
60
48
36
24
12
0
2 d
2 w
3 mo
12 mo
5 d
12 mo
CA1
sp
sr
so
sp
sr
C
E
NCx
D
F

Figure 4

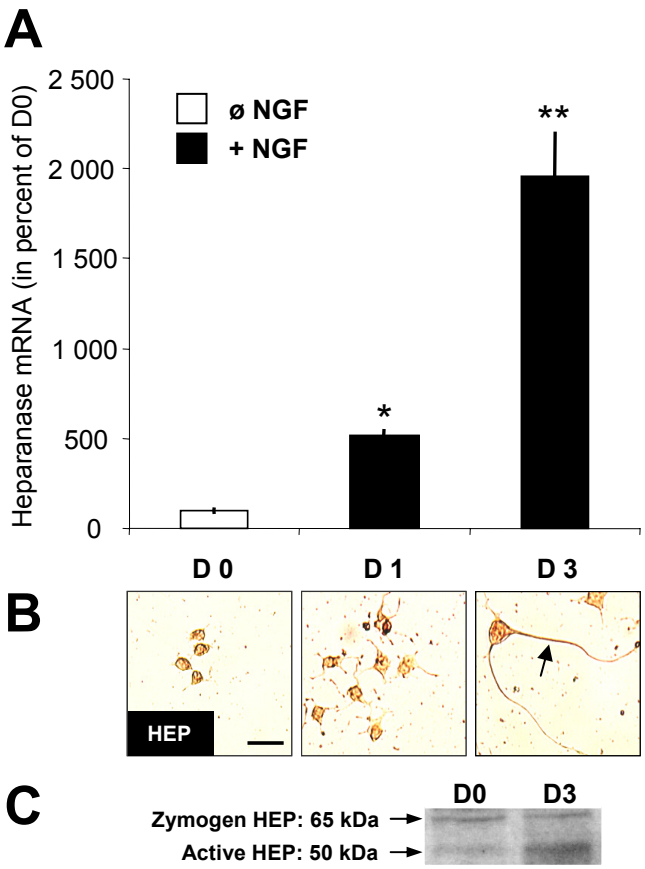
A
Heparanase mRNA (in percent of D0)
2 500
2 000
1 500
1 000
500
0
ø NGF
+ NGF
*
**
D 0
D 1
D 3
B
HEP
C
D0
D3
Zymogen HEP: 65 kDa
Active HEP: 50 kDa

Figure 5

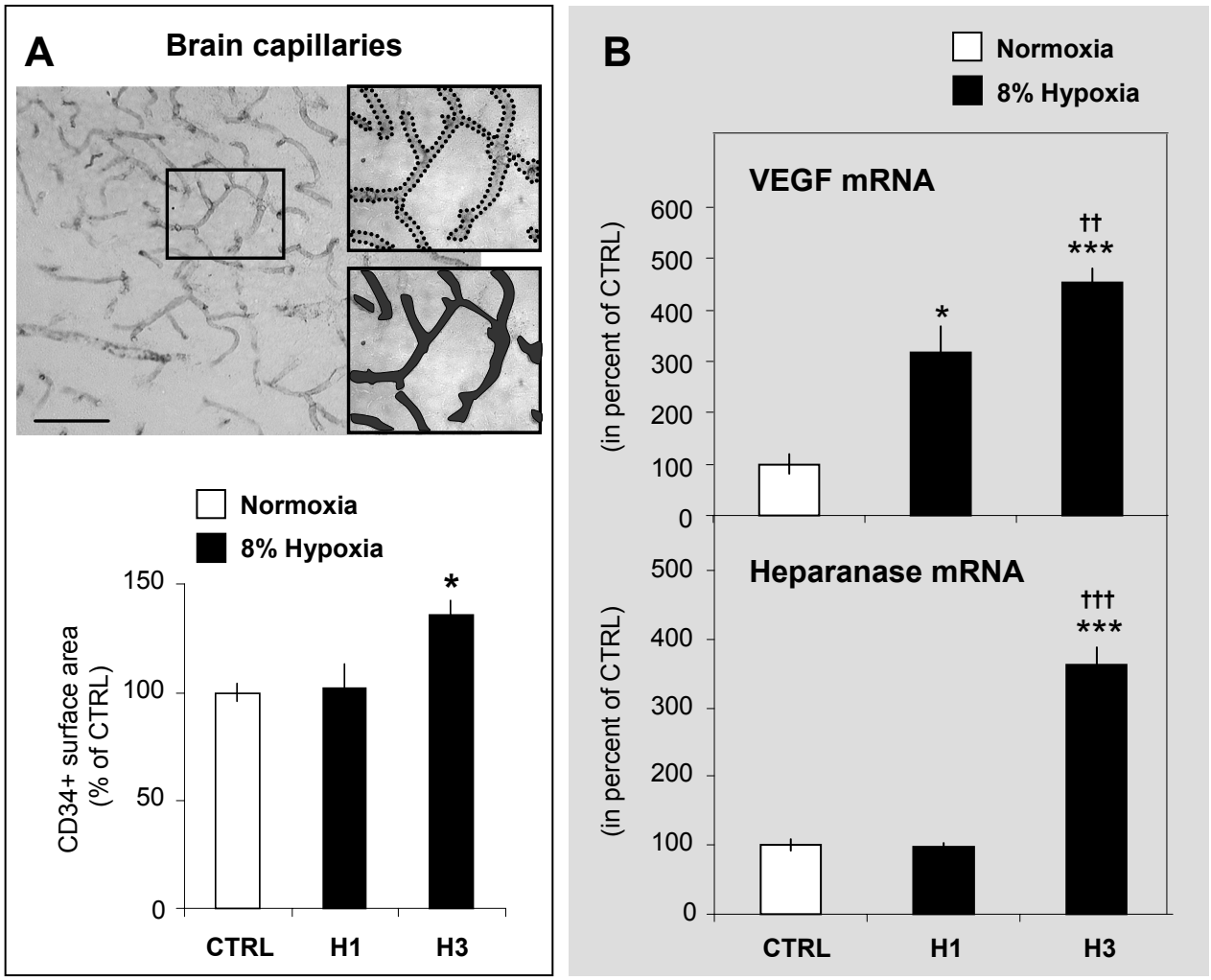
A
Brain capillaries
Normoxia
8% Hypoxia
CD34+ surface area
(% of CTRL)
150
100
50
0
*
CTRL
H1
H3
B
Normoxia
8% Hypoxia
VEGF mRNA
(in percent of CTRL)
600
500
400
300
200
100
0
*
††
***
Heparanase mRNA
(in percent of CTRL)
500
400
300
200
100
0
†††
***
CTRL
H1
H3

Figure 6

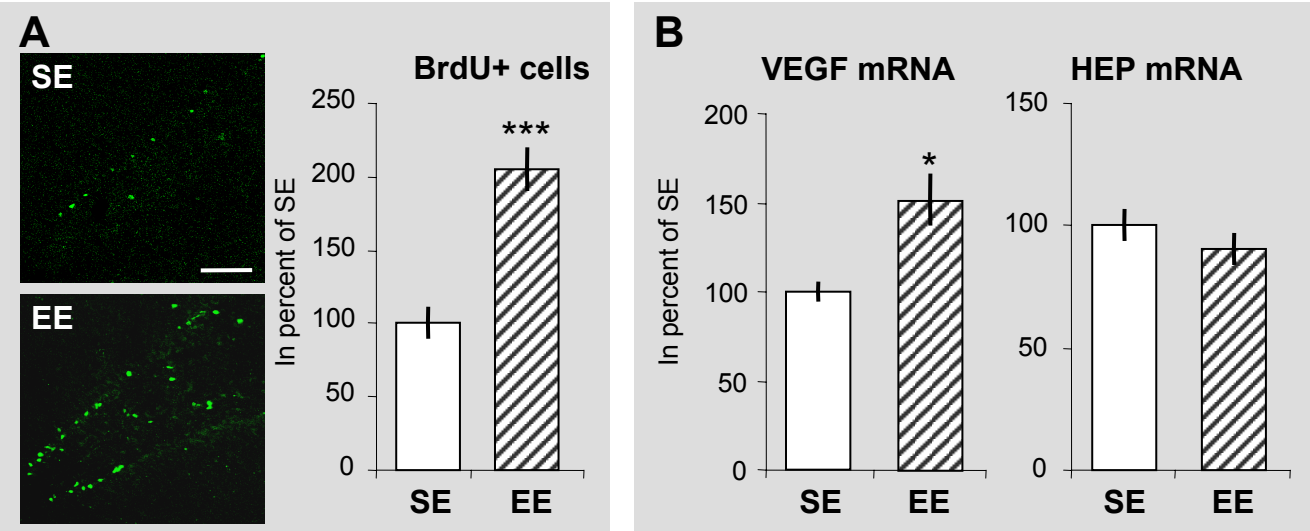
A
SE
EE
BrdU+ cells
In percent of SE
250
200
150
100
50
0
***
SE
EE
B
VEGF mRNA
HEP mRNA
In percent of SE
200
150
100
50
0
*
150
100
50
0
SE
EE
SE
EE

Figure 7